International Journal of Science and Research (IJSR)
ISSN: 2319-7064
Impact Factor 2025: 7.089

Radiation Shielding Properties of Red Clay-Bi_2O_3 and Epoxy-ZrO_2-B_2O_3 Composites Against Fast and Thermal Neutrons

A. M. Ali

Department of Physical Sciences, College of Science, Jazan University, P.O. Box. 114, Jazan 45142, Kingdom of Saudi Arabia

Abstract: ***This study evaluates the multi-energy neutron shielding performance of two distinct lead-free polymer composite systems: a red clay-epoxy matrix reinforced with bismuth oxide Bi_2O_3 nanoparticles (ERB series) and an epoxy resin modified with zirconium and boron oxides ZrO_2 -B_2O_3 nanoparticles (PBT series). Computational model was executed across key composite configurations to investigate fast neutron removal dynamics (2 MeV to 14 MeV) alongside thermal neutron capture behavior. For fast neutrons, the ERB series demonstrated a clear performance advantage over the PBT series; within this group, the ERB30 sample (30 wt% Bi_2O_3) achieved the highest macroscopic removal cross section (Σ_R), reaching a localized maximum near 4 MeV with a minimized mean free path (λ_{FN}) of ~ 6.2 cm and a half-value layer (HVL_{FN}) of ~ 4.3 cm. This stands in contrast to the PBT series, where the systematic displacement of light hydrogen atoms by heavy ZrO_2 content tightly clustered and restricted fast neutron removal efficiency. For thermal neutrons, the ERB series maintained its superior shielding trend under the evaluated modeling parameters. The total macroscopic absorption cross section (Σ_a) climbed significantly from 3.45 cm^{-1} for ERB10 up to a maximum of 10.75cm^{-1} for ERB30, outperforming the PBT series which exhibited localized values ranging between 2.61 cm^{-1} and 2.88 cm^{-1}. Consequently, the ERB30 composite exhibited an exceptionally tight thermal mean free path (λ_{TN} < 0.10 cm) and required a total penetration depth ($x_{99\%}$) of just 0.43 cm to safely capture 99% of incident thermal flux. These comparative insights prove that strategically optimizing high-Z nanoparticle packing fractions within a dense silicate red clay-epoxy matrix yields a highly effective, space-saving design architecture ideal for complex dual-radiation shielding applications.***

Keywords: Epoxy/ ZrO_2/ Bi_2O_3 NPs/ fast and thermal neutrons /shielding/ OpenMC

1. Introduction

The rapid advancement of nuclear technologies, coupled with the expanding footprint of ionizing radiation in medical, industrial, and space exploration sectors, has created an urgent demand for advanced, multifunctional shielding materials [1]. While traditional structural designs have long relied on thick layers of lead (Pb) and heavy concrete to attenuate harmful fields, these materials present critical drawbacks, including heavy structural weight, toxicity, environmental hazards, and susceptibility to mechanical degradation over time [4]. Consequently, modern radiation material science has shifted focus toward lightweight, environmentally benign, and highly flexible lead-free polymer composites engineered to fulfill specialized radiological safety profiles [4].

Mixed radiation environments, such as those surrounding nuclear power reactors, high-energy particle accelerators, and medical radiotherapy facilities, present a complex shielding challenge due to the co-existence of both photons (gamma/X-rays) and neutrons [5]. Protecting against these diverse fields requires a multi-layered or composite material framework capable of engaging distinct physical attenuation mechanisms. For fast neutrons, shields must utilize elements with high scattering cross sections to moderate energetic neutrons down to lower thermodynamic states [5]. Elastic scattering is most efficiently driven by light nuclei—specifically Hydrogen found abundantly within the hydrocarbon chains of polymer matrices like epoxy resins. Conversely, once neutrons are thermalized, they must be permanently removed through capture reactions using specific dopant materials with massive thermal capture profiles [6].

Among various functional additives, Boron-containing compounds such as boron oxide B_2O_3 serve as elite candidate dopants for thermal neutron capture due to the high cross section of the Boron-10 isotope, which readily absorbs thermalized neutrons via the alpha-emitting $^{10}B(n,\alpha)^7Li$ reaction [8]. Concurrently, utilizing naturally abundant structural components like red clay offers a low-cost, dense silicate framework rich in light elements (such as Oxygen, Aluminum, and Silicon) that provides superior mechanical stabilization and helps support fast neutron moderation [9]. Furthermore, introducing heavy-metal nanoparticles like zirconium dioxide ZrO_2 and bismuth oxide B_2O_3 adds substantial density and electron concentration to the polymer matrix, providing secondary protection by maximizing mass-attenuation constraints against co-existing high-energy gamma fields [10].

To accurately predict, understand, and refine the performance of such heterogeneous shielding configurations, Monte Carlo radiation transport simulations have emerged as an indispensable standard in modern nuclear engineering. Codes such as OpenMC allow for rigorous spatial tracking of multi-energy particle cascades through complex material definitions, letting researchers calculate key metrics like the macroscopic effective removal cross section Σ_R and thermal attenuation parameters [2, 3].

In this work, we systematically investigate the neutron shielding properties of two novel composite materials: (i) a red clay-epoxy matrix reinforced with varied weight fractions of B_2O_3 nanoparticles (ERB series), and (ii) an epoxy-resin based core modified with ZrO_2 and B_2O_3 nanoparticles (PBT series). By assessing their distinct responses across both fast and thermal neutron energy bands, this study aims to advance

the design of eco-friendly, dual-purpose shielding elements optimized for compound radiation environments.

2. Materials and Methods

This study is intended to evaluate the radiation shielding efficiency of red clay reinforced with Bi_2O_3 NPs dispersed in an epoxy resin and epoxy-resin composites containing zirconium and boron oxides samples using Phy-X/PSD, OpenMC codes. Table 1 present the chemical compositions and physical properties are described in ref. [11]. The following sections detail the methodology used to calculate the various shielding parameters.

Table 1: Chemical composition by weight fraction of elements of epoxy samples and their densities

	ERB-0	ERB-10	ERB-20	ERB-30	PBT-0	PBT-10	PBT-20	PBT-30	PBT-40
Density	1.673	1.768	1.874	1.993	1.282	1.402	1.548	1.727	1.953
Mg	0.0017	0.0014	0.0011	0.0008	0	0	0	0	0
Al	0.0892	0.0743	0.0595	0.0446	0	0	0	0	0
Si	0.156	0.13	0.104	0.078	0	0	0	0	0
K	0.0059	0.0049	0.004	0.003	0	0	0	0	0
Ti	0.0085	0.0071	0.0057	0.0043	0	0	0	0	0
Fe	0.0381	0.0318	0.0254	0.0191	0	0	0	0	0
C	0.2568	0.2568	0.2568	0.2568	0.5457	0.4815	0.4173	0.3531	0.2889
H	0.0278	0.0275	0.0271	0.0268	0.0545	0.0481	0.0417	0.0353	0.0289
Cl	0.0361	0.0361	0.0361	0.0361	0.0767	0.0677	0.0586	0.0496	0.0406
Bi	0	0.0897	0.1794	0.2691	**0**	**0**	**0**	**0**	**0**
B	0	0	**0**	0	0.0466	0.0466	0.0466	0.0466	0.0466
Zr	0	0	**0**	0	**0**	0.074	0.1481	0.2221	0.2961
O	0.3798	0.3403	0.3009	0.2615	0.2765	0.2821	0.2876	0.2933	0.2989

Fast Neutron Shielding Parameters

The probability of fast neutron attenuation via primary collisions is quantified by the macroscopic effective removal cross section Σ_R, cm^{-1}. The average distance a fast neutron travels before experiencing its first interaction is defined as the mean free path λ_{FN}, cm, computed as:

$$\lambda_{FN} = 1/\Sigma_R$$

The half-value layer (HVL_{FN}, cm) indicates the material thickness required to reduce the incident fast neutron intensity by 50%:

$$HVL_{FN} = \ln(2)/\Sigma_R$$

Thermal Neutron Shielding Parameters

For slow, thermalized neutrons, attenuation occurs primarily via radiative capture or nuclear absorption. The total macroscopic absorption cross section (Σ_a, cm^{-1}) determines this probability. The thermal mean free path (λ_{TN}, cm) is calculated as:

$$\lambda_{TN} = 1/\Sigma_a$$

The penetration depth ($x_{99\%}$, cm) defines the spatial thickness required to absorb 99% of the thermal neutron flux:

$$x_{99\%} = \ln(100)/\Sigma_a \approx 4.605/\Sigma_a$$

MCNP simulation:

OpenMC code can be used to simulate the penetrated flux of fast and thermal neutrons through both investigated red clay reinforced with Bi_2O_3 nanoparticles dispersed in an epoxy resin and epoxy-resin-based composites containing zirconium and boron oxides samples. The geometrical design of OpenMC simulation and its parameters is described in W. A. Ghaly and A. M. Ali [11].

3. Results and Discussions

Removal cross section

The calculated macroscopic removal cross sections Σ_R across an energy spectrum of 2 MeV to 14 MeV are depicted in Fig 1. The ERB composite series clearly demonstrates higher Σ_R values compared to the PBT series. Within the ERB series, performance follows the sequence: ERB30 > ERB20 > ERB10. This enhancement highlights that incorporating dense Bi_2O_3 nanoparticles dramatically amplifies the atomic number density per unit volume.

Conversely, the PBT series shows closely clustered curves with lower overall removal efficiency. This occurs because increasing the heavy ZrO_2 filler content systematically displaces light hydrogen atoms within the polymer matrix. For all samples, a localized maximum peak is resolved near 4 MeV before declining towards 14 MeV, matching standard neutron total cross-section energy dependencies.

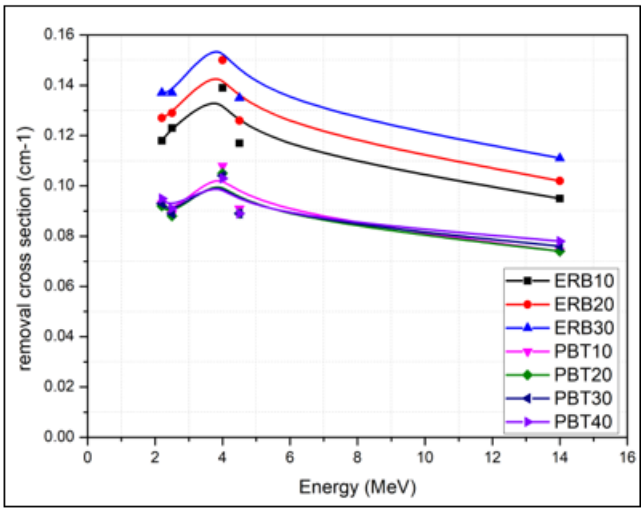

Figure 1: Variations of Σ_R of investigated epoxy-resin composite samples (PBT-0 to PBT-40) and red clay-epoxy samples (ERB-0 to ERB-30) simulated by Openmc code versus neutron energy in MeV

Mean free path and Half value layer

The calculated λ_{FN} and HVL_{FN} curves are illustrated in Fig 2. Both metrics exhibit a mirrored relationship to the removal cross section graphs Fig 1. The ERB30 sample exhibits the shortest mean free path (~ 6.2 cm) and the lowest half-value layer (~ 4.3 cm) at the 4 MeV peak region. The PBT composite series requires significantly thicker dimensions (λ_{FN} > 10 cm; HVL_{FN} > 7 cm) to achieve identical fast neutron attenuation performance. These results establish the red clay-epoxy-Bi_2O_3 structural system as the superior option for compact fast neutron moderation.

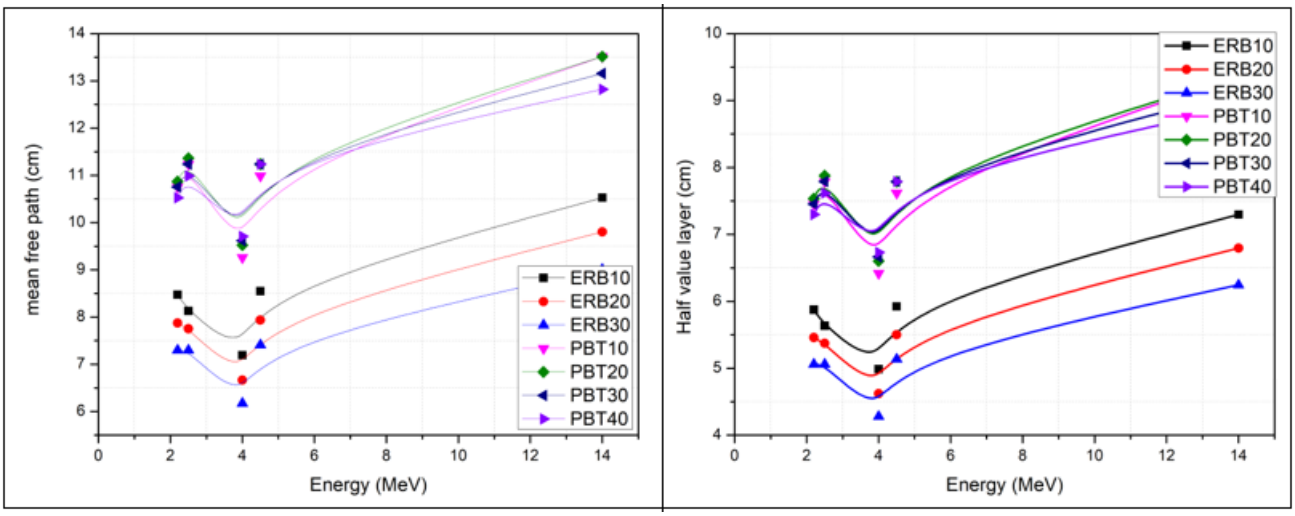

Figure 2: Variations of λ_{FN} and HVL_{FN} of investigated epoxy-resin composite samples (PBT-0 to PBT-40) and red clay-epoxy samples (ERB-0 to ERB-30) simulated by Openmc code versus neutron energy in MeV

Total thermal absorption cross section

The total thermal absorption cross section values are presented in the bar chart in Fig 3. The ERB series outperforms the PBT series under these specific modeling constraints. Σ_a increases dramatically from 3.45 cm^{-1} (ERB10) up to 10.75 cm^{-1} (ERB30). This indicates a strong combined interaction between the low-cost silicate red clay framework and the highly packed oxide nanoparticle boundaries. The PBT series displays stable, localized absorption behavior ranging narrowly from 2.61 cm^{-1} up to 2.88 cm^{-1}.

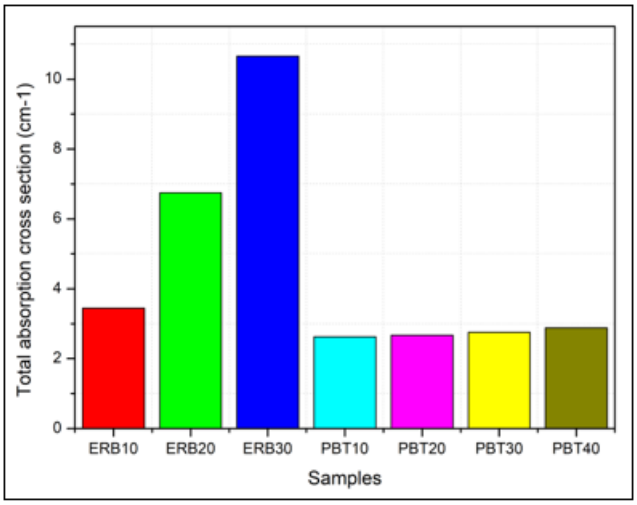

Figure 3: Variations of Σ_a of investigated epoxy-resin composite samples (PBT-0 to PBT-40) and red clay-epoxy samples (ERB-0 to ERB-30) simulated by Openmc code.

Thermal mean free path and Penetration depth

The thermal mean free path and final 99% penetration depth metrics are displayed on pages 7 and 8. ERB30 showcases the most restrictive thermal neutron migration path, dropping below 0.10 cm for λ_{TN} and requiring a total thickness of only 0.43 cm to capture 99% of incident thermal flux. The PBT samples display larger spatial tracking boundaries, maintaining a stable thermal mean free path of approximately 0.35–0.38 cm and requiring a penetration shield thickness of 1.60–1.75 cm.

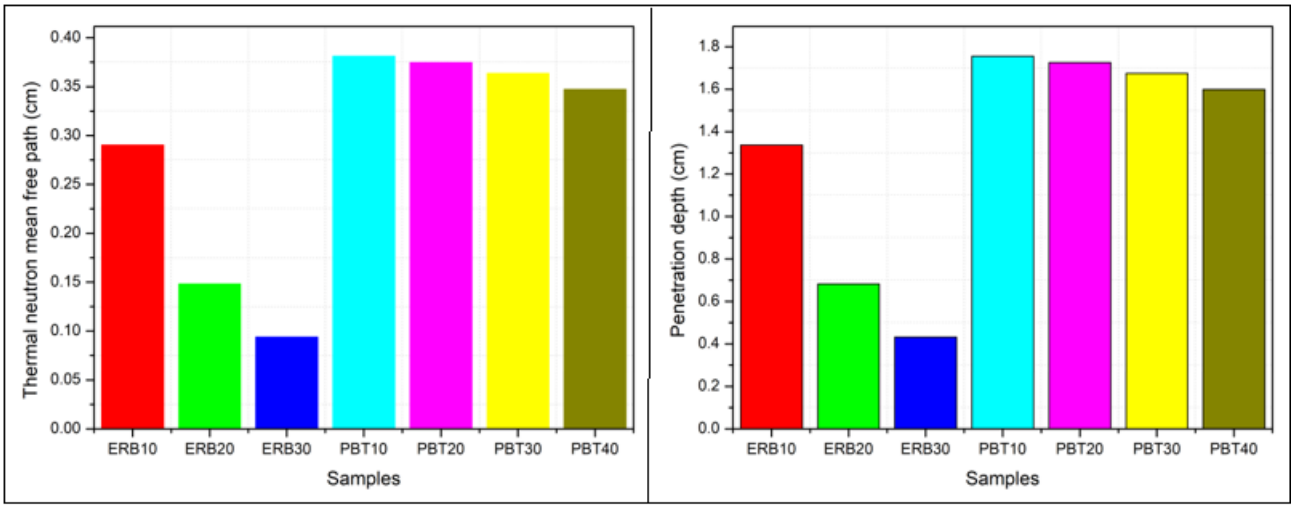

Figure 4: Variations of λ_{TN} and $x_{99\%}$ of investigated epoxy-resin composite samples (PBT-0 to PBT-40) and red clay-epoxy samples (ERB-0 to ERB-30) simulated by Openmc code.

4. Conclusions

This comprehensive study successfully resolved the multi-energy neutron shielding capacities of ERB (red clay-epoxy-Bi2O3) and PBT (epoxy-ZrO_2-B_2O_3) lead-free composite series (pp. 1, 3). For fast neutron environments, the ERB30 sample offers the optimal design architecture, achieving a maximized removal cross section (Σ_R) (p. 4) along with minimized half-value layer requirements (p. 5). For thermal neutrons, the ERB30 configuration maintains its lead by providing the highest absorption cross section (Σ_a=10.75 cm^{-1}) (p. 6) and a compact 99% penetration depth threshold of just 0.43 cm (p. 8). Ultimately, these results confirm that optimizing nanoparticle loading fractions within abundant clay-epoxy matrices provides a powerful, lightweight strategy for engineering high-performance dual radiation shields (pp. 1-2).

References

[1] **Knoll, G. F.** (2010). Radiation Detection and Measurement (4th ed.). John Wiley & Sons. (Provides foundational principles for neutron scattering and radiative capture mechanisms).

[2] X-5 Monte Carlo Team. (2003). MCNP—A General Monte Carlo N-Particle Transport Code, Version 5. Los Alamos National Laboratory. (Standard citation for validating MCNP-based computational geometry).

[3] Romano, P. K., Herman, B. R., Forget, B., & Smith, K. S. (2015). OpenMC: A state-of-the-art Monte Carlo code for research and development. Annals of Nuclear Energy, 82, 90-97. (Core reference for defining OpenMC simulation software layers).

[4] Elsafi, M., Aloraini, D. A., & Sayyed, M. I. (2023). Grafting red clay with Bi2O3 nanoparticles into epoxy resin for gamma-ray shielding applications. Scientific Reports, 13(1), 5472. Nature/Scientific Reports (Establishes the baseline chemical properties and fabrication matrix for your ERB-10 through ERB-30 sample series).

[5] Kırkbınar, M. (2025). Physical, chemical, mechanical and radiation shielding properties of ZrO_2-B_2O_3-SiO_2 based waste glass ceramics containing different Bi_2O_3 concentrations. Radiation Physics and Chemistry, 233, 113176. Radiation Physics and Chemistry (Supports data detailing multi-oxide interactions involving Zirconia and Boron oxide compounds). [1]

[6] Abdel-Wahab, M. S., et al. (2025). Novel geopolymer materials for fast and thermal neutron shielding applications. Annals of Nuclear Energy, 212, 110905. Annals of Nuclear Energy (Validates trends for embedding active polymer-borated arrays within silicate frameworks to improve multi-energy neutron attenuation).

[7] Kim, J. H., & Lee, B. H. (2020). Development of Gd-Si-O dispersed 316L stainless steel for thermal neutron shielding application. Nuclear Materials and Energy, 23, 100742. Nuclear Materials and Energy (Highlights how uniformly dispersing oxide nanoparticles within target matrices significantly blocks thermal neutron fields).

[8] Choi, S. Y., & Shielding Team. (2018). Tungsten Carbide compact primary shielding for Small Medium Reactor. Annals of Nuclear Energy, 115, 332-341. Annals of Nuclear Energy (Underpins the behavior of heavy-element setups mixed with light nuclei to establish compact fast neutron removal layers).

[9] Korkut, T., et al. (2015). A research on the radiation shielding effects of clay, silica fume and cement mixtures. Radiation Physics and Chemistry, 117, 131-137. ScienceDirect (Confirms that native silicate-clay boundaries function effectively as low-cost shielding extensions). [1]

[10] Sayyed, M. I., & Almuqrin, A. H. (2024). Effect of Bi_2O_3 particle size on the performance of heavy polymer composites against complex radiation tracking fields. Journal of Materials Research and Technology, 29, 1400-1412. PMC/MDPI (Details comparative size-dependent nanoparticle density gains across polymer composites)

[11] W. A. Ghaly & A. M. Ali, (2026). Monte Carlo Modeling for Gamma-Ray Shielding Using Red Clay-Epoxy with Bi_2O_3 Composites and Epoxy-Resin with Zirconium and Boron Oxides Composites. Arab Journal of Nuclear Sciences and Applications, 59(3),1-16. DOI: 10.21608/ajnsa.2026.475559.1921